

Highly-accurate Computation of Supersonic Flows around a Concave Body (II. Motion analysis by moving-coordinate method)

Masayuki Nomura¹ & Yoko Takakura²

^{1,2} Department of Prime Mover Engineering, Tokai University, Kanagawa 259-1292, Japan

Corresponding author: takakura@tokai-u.jp

Abstract: The moving-coordinate method presented by the authors is a methodology where physical phenomena are observed from the accelerating frame attached to a moving body. In this study, the moving-coordinate method is generalized by newly including both the translational and rotational motions of the frame. The source terms are derived for momentum and energy equations and the transformations of momentum and total energy between the inertial frame and the moving frame are presented. As the moving body is observed to be stationary in the moving-coordinate method, the present method has advantages that there is no regeneration of the grid around the object and no calculation error induced by moving grids. The present method was applied to supersonic flows around a rectangular parachute model, and the results showed the self-excited motions of the model.

Keywords: Moving-coordinate method, Supersonic parachute, Self-excited motion

1 Introduction

Supersonic parachutes are effective aerodynamic decelerators for atmospheric entry vehicles. They have been used so many times in the re-entry of planetary probes because of advantages of their high drag force with light weight, and simple structure compactly storable. However, they have flexibility and there occur the shock-vortex interactions in the complicated flow field, and therefore their aerodynamic characteristics and the trajectory of their motion are still incompletely understood.

In the wind tunnel experiments with hemispherical and rigid parachute model [1, 2], it is reported that the detached shock wave in front of the model vibrates. The vibration tends to occur as the Mach number becomes higher. The vibration sometimes occurs after the pressure waves go and return between the detached shock wave and the inside of the model, and, even if the vibration once continue, the flow phenomena return to quasi-steady states again. The shock-vibration is a distinctive phenomenon in the supersonic parachute experiments, but the details of the mechanism have not been clarified yet.

Takakura et al. [3] carried out computations of supersonic flows using high accuracy WENO schemes about a rectangular concave body as the parachute model, and reported: when the disturbance of Mach number is added to the uniform flow, the feedback phenomenon occurs with vortices and pressure waves, where the vortices released from the central part of the detached shock wave are advected downstream toward the inside and edge of the concave body, and the pressure waves generated

¹ Present: Graduate School of Tohoku University

by the interaction of the vortices with the edge propagates upstream. They mentioned the possibility that this feedback may cause the asymmetric vibration of the shock waves. However, these released vortices were captured too largely on coarse grid portion at the shock wave, and afterward re-computations on the grids with high resolution of shock waves were reported [4, 5] in detail about generation of the sound waves at the edge of the concave body and the vortex release from the detached shock wave. It is indicated that the pressure waves propagate downstream and upstream between the bottom of the concave body and the detached shock wave firstly when the disturbance is given.

Hatanaka, et al. [6] performed three-dimensional numerical computations around a rigid hemispherical shell in supersonic flows and reproduced the phenomenon observed in the wind tunnel experiments by Kawamura and Mizukaki [2]. They showed that the frequency of the small-scale vibration of the detached shock wave can be explained by the cavity resonance based on the distance between the bottom of the hemispherical shell and the detached shock wave.

In the above researches, the parachute model have been treated as rigid and not in motion, however the actual parachute moves around a pivot. As such unsteady self-excited motion makes prediction of the moving direction of the object difficult, analysis of self-excited motion and research of numerical methods for flow field around a moving object are being conducted.

Yamakawa and Matsuno [7] applied finite-volume method on an unstructured moving grid to compressible flows and showed effectiveness and extensibility of the scheme by computation of the piston problem and the gun tunnel problem. Inomoto and Matsuno [8] applied finite-volume method on an unstructured moving grid to incompressible flow and showed that the scheme is effective to coupled analysis of fluid dynamics and kinematics to reproduce behaviour of a blow ball.

Flows around a moving body are computed numerically on moving grids in most cases. On the contrary, the moving-coordinate method presented by the authors [9] is to fix the coordinate system to a moving body, where the moving body stands still with stationary grids. Authors [10] derived moving-coordinate method systematically from the governing equations of compressible flow in general-coordinate system, and applied it to numerical computations of the flow field inside the ballistic range at launch of the flying object and the flow in the opening operation of high-voltage gas insulated circuit breaker. The moving-coordinate method has advantages that it is not necessary to reconstruct the grid around an object when the object moves, and there is no calculation error caused by grid movement.

In [10] the moving frame had only translational velocity relative to the standard inertial frame. Here the moving-coordinate method is extended to have the translational and rotational motions. The governing equations are derived for the generalized moving-coordinate method, and the present method is applied to supersonic flows around a rectangular parachute model.

2 Moving-coordinate method

The moving-coordinate method is a method to observe the flow field from a coordinate system attached to the body in motion. Consider a standard-coordinate system I (inertial frame) and a moving-coordinate system A (accelerating frame) accelerating with regard to it [11], which is carrying out a translation with relative velocity V_0 and a rotation with angular vector Ω as shown in Fig. 2.1. Let \mathbf{r} be the position vector for the origin of the accelerating frame in system I, and \mathbf{x} be the position vector in system A, then fluid velocity \mathbf{u} at position $\mathbf{r}+\mathbf{x}$ observed from the standard-coordinate system I and fluid velocity \mathbf{u}_* at position \mathbf{x} observed from the moving-coordinate system A have the following relation:

$$\begin{aligned}\mathbf{u} - \mathbf{V}_G &= \mathbf{u}_* , & \mathbf{V}_G &= \mathbf{V}_0 + \Omega \times \mathbf{x} \\ \mathbf{u} &= \mathbf{u}_* + \mathbf{V}_0 + \Omega \times \mathbf{x}\end{aligned}\tag{2.1}$$

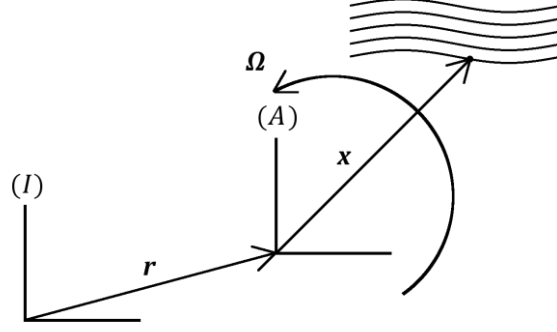


Figure 2.1: Moving-coordinate frame (A) with translation and rotation.

In this section, first, we describe the basic fluid equations in Lagrangian notation, and then, we will derive those on moving-coordinate frame. In the notation below, $\rho, E, p, \mathbf{T}, \mathbf{q}$ are the density, the total energy per unit volume, the pressure, the viscous stress tensor, the heat flux vector, respectively.

2.1 Continuity equation

The continuity equation in the standard-coordinate system can be written as follows:

$$\begin{aligned} \frac{\partial \rho}{\partial t} + \nabla \cdot (\rho \mathbf{u}) &= 0 \\ \frac{D\rho}{Dt} + \rho \nabla \cdot \mathbf{u} &= 0 \end{aligned} \quad (2.2)$$

Substituting Eq. (2.1) into Eq. (2.2) leads to

$$\frac{D\rho}{Dt} + \rho \nabla \cdot \mathbf{u}_* + \rho \nabla \cdot \mathbf{V}_0 + \rho \nabla \cdot (\boldsymbol{\Omega} \times \mathbf{x}) = 0$$

Since $\rho \nabla \cdot \mathbf{V}_0 = 0$ and $\rho \nabla \cdot (\boldsymbol{\Omega} \times \mathbf{x}) = 0$, we obtain continuity equation in the moving-coordinate system:

$$\frac{D\rho}{Dt} + \rho \nabla \cdot \mathbf{u}_* = 0 \quad (2.3)$$

Thus, it was shown that the continuity equation is unchanged between the coordinate systems I and A.

2.2 Equation of motion

The equation of motion in the standard-coordinate system can be written as follows:

$$\rho \frac{D\mathbf{u}}{Dt} = -\nabla p + \nabla \cdot \mathbf{T} \quad (2.4)$$

In the moving-coordinate system moving with an acceleration to the inertial frame, using the unit normal bases, $\mathbf{e}_1, \mathbf{e}_2, \mathbf{e}_3$, an arbitrary vector \mathbf{b} is expressed as

$$\mathbf{b} = b_1 \mathbf{e}_1 + b_2 \mathbf{e}_2 + b_3 \mathbf{e}_3 = b_i \mathbf{e}_i$$

The rate of change of \mathbf{b} observed in the inertial frame is written as follows:

$$\left[\frac{D\mathbf{b}}{Dt}\right]_I = \frac{Db_i}{Dt}\mathbf{e}_i + b_i \frac{D\mathbf{e}_i}{Dt}, \quad \frac{D\mathbf{e}_i}{Dt} = \boldsymbol{\Omega} \times \mathbf{e}_i$$

Therefore the following relation between the inertial and accelerating frames is derived [11]:

$$\left[\frac{D\mathbf{b}}{Dt}\right]_I = \left[\frac{D\mathbf{b}}{Dt}\right]_A + \boldsymbol{\Omega} \times \mathbf{b} \quad (2.5)$$

where subscripts I and A denote the inertial frame and the accelerating frame, respectively. Differentiating Eq. (2.1) with respect to the inertial frame and using Eq. (2.5) and $[D\mathbf{x}/Dt]_A = \mathbf{u}_*$:

$$\left[\frac{D\mathbf{u}}{Dt}\right]_I = \underbrace{\left[\frac{D\mathbf{u}_*}{Dt}\right]_I}_i + \left[\frac{DV_0}{Dt}\right]_I + \underbrace{\left[\frac{D(\boldsymbol{\Omega} \times \mathbf{x})}{Dt}\right]_I}_{ii} \quad (2.6)$$

In the right hand side, the first and third terms can be transformed into the accelerating frame by use of Eq. (2.5):

$$i. \quad \left[\frac{D\mathbf{u}_*}{Dt}\right]_I = \left[\frac{D\mathbf{u}_*}{Dt}\right]_A + \boldsymbol{\Omega} \times \mathbf{u}_*$$

$$ii. \quad \begin{aligned} \left[\frac{D(\boldsymbol{\Omega} \times \mathbf{x})}{Dt}\right]_I &= \left[\frac{D(\boldsymbol{\Omega} \times \mathbf{x})}{Dt}\right]_A + \boldsymbol{\Omega} \times (\boldsymbol{\Omega} \times \mathbf{x}) \\ &= \boldsymbol{\Omega} \times \left[\frac{D\mathbf{x}}{Dt}\right]_A + \left[\frac{D\boldsymbol{\Omega}}{Dt}\right]_A \times \mathbf{x} + \boldsymbol{\Omega} \times (\boldsymbol{\Omega} \times \mathbf{x}) \\ &= \boldsymbol{\Omega} \times \mathbf{u}_* + \left[\frac{D\boldsymbol{\Omega}}{Dt}\right]_A \times \mathbf{x} + \boldsymbol{\Omega} \times (\boldsymbol{\Omega} \times \mathbf{x}) \end{aligned}$$

Thus Eq. (2.6) is expressed as:

$$\left[\frac{D\mathbf{u}}{Dt}\right]_I = \left[\frac{D\mathbf{u}_*}{Dt}\right]_A + \frac{dV_0}{dt} + 2(\boldsymbol{\Omega} \times \mathbf{u}_*) + \boldsymbol{\Omega} \times (\boldsymbol{\Omega} \times \mathbf{x}) + \frac{d\boldsymbol{\Omega}}{dt} \times \mathbf{x} \quad (2.7)$$

Substituting Eq. (2.7) into Eq. (2.4) and rearranging it, we can obtain equation of motion in the moving-coordinate system [11]:

$$\rho \left[\frac{D\mathbf{u}_*}{Dt}\right]_A = (-\nabla p + \nabla \cdot \mathbf{T}) - \rho \left\{ \underbrace{\frac{dV_0}{dt}}_{\text{translational acceleration}} + \underbrace{2(\boldsymbol{\Omega} \times \mathbf{u}_*)}_{\text{Coriolis's force}} + \underbrace{\boldsymbol{\Omega} \times (\boldsymbol{\Omega} \times \mathbf{x})}_{\text{centrifugal force}} + \underbrace{\frac{d\boldsymbol{\Omega}}{dt} \times \mathbf{x}}_{\text{unsteady term}} \right\} \quad (2.8)$$

2.3 Energy equation

The Energy equation in the standard-coordinate system is written as follows:

$$\rho \frac{D(E/\rho)}{Dt} = \underbrace{-\nabla \cdot (p\mathbf{u}) + \nabla \cdot (\mathbf{T} \cdot \mathbf{u})}_{iii} - \nabla \cdot \mathbf{q} \quad (2.9)$$

Now we describe the total energy E in the standard-coordinate system by using the total energy E_* in

the moving-coordinate system:

$$E = \frac{p}{\gamma - 1} + \frac{1}{2}\rho \mathbf{u} \cdot \mathbf{u} \quad (2.10)$$

$$E_* = \frac{p}{\gamma - 1} + \frac{1}{2}\rho \mathbf{u}_* \cdot \mathbf{u}_* \quad (2.11)$$

By substituting Eq. (2.1) for Eq. (2.10)

$$E = \frac{p}{\gamma - 1} + \frac{1}{2}\rho(\mathbf{u}_* + \mathbf{V}_0 + \boldsymbol{\Omega} \times \mathbf{x}) \cdot (\mathbf{u}_* + \mathbf{V}_0 + \boldsymbol{\Omega} \times \mathbf{x})$$

and further by using Eq. (2.1), the following equatin is obtained.

$$E = E_* + \rho \mathbf{u}_* \cdot (\mathbf{V}_0 + \boldsymbol{\Omega} \times \mathbf{x}) + \frac{1}{2}\rho(\mathbf{V}_0 + \boldsymbol{\Omega} \times \mathbf{x}) \cdot (\mathbf{V}_0 + \boldsymbol{\Omega} \times \mathbf{x}) \quad (2.12)$$

Eq. (2.12) is divided by ρ and differentiated with respect to the inertial frame:

$$\frac{D(E/\rho)}{Dt} = \frac{D(E^*/\rho)}{Dt} + \underbrace{\left[\frac{D}{Dt} \{ \mathbf{u}_* \cdot (\mathbf{V}_0 + \boldsymbol{\Omega} \times \mathbf{x}) \} \right]_I}_{\text{iv.}} + \frac{1}{2} \underbrace{\left[\frac{D}{Dt} \{ (\mathbf{V}_0 + \boldsymbol{\Omega} \times \mathbf{x}) \cdot (\mathbf{V}_0 + \boldsymbol{\Omega} \times \mathbf{x}) \} \right]_I}_{\text{v.}} \quad (2.13)$$

Here the first term in the right hand side of Eq. (2.9) can be written, using the velocity transformation between frames (2.1) and unit matrix \mathbf{I} , as follows:

$$\begin{aligned} \text{iii.} \quad -\nabla \cdot (p\mathbf{u}) + \nabla \cdot (\mathbf{T} \cdot \mathbf{u}) &= \nabla \cdot \{ (-p\mathbf{I} + \mathbf{T}) \cdot \mathbf{u} \} \\ &= \nabla \cdot \{ (-p\mathbf{I} + \mathbf{T}) \cdot (\mathbf{u}_* + \mathbf{V}_0 + \boldsymbol{\Omega} \times \mathbf{x}) \} \\ &= \nabla \cdot \{ (-p\mathbf{I} + \mathbf{T}) \cdot \mathbf{u}_* \} + \nabla \cdot \{ (-p\mathbf{I} + \mathbf{T}) \cdot (\mathbf{V}_0 + \boldsymbol{\Omega} \times \mathbf{x}) \} \\ &= \nabla \cdot \{ (-p\mathbf{I} + \mathbf{T}) \cdot \mathbf{u}_* \} + \{ \nabla \cdot (-p\mathbf{I} + \mathbf{T}) \} \cdot (\mathbf{V}_0 + \boldsymbol{\Omega} \times \mathbf{x}) \\ &\quad (\because \nabla \cdot (\mathbf{V}_0 + \boldsymbol{\Omega} \times \mathbf{x}) = 0) \end{aligned}$$

The second and third terms in the right hand side of Eq. (2.13) can be rewritten, using the equation of motion, as follows:

$$\begin{aligned} \text{iv.} \quad \left[\frac{D}{Dt} \{ \mathbf{u}_* \cdot (\mathbf{V}_0 + \boldsymbol{\Omega} \times \mathbf{x}) \} \right]_I &= \mathbf{u}_* \cdot \left[\frac{D}{Dt} (\mathbf{V}_0 + \boldsymbol{\Omega} \times \mathbf{x}) \right]_I + \left[\frac{D\mathbf{u}_*}{Dt} \right]_I \cdot (\mathbf{V}_0 + \boldsymbol{\Omega} \times \mathbf{x}) \\ &= \mathbf{u}_* \cdot \left[\frac{D}{Dt} (\mathbf{V}_0 + \boldsymbol{\Omega} \times \mathbf{x}) \right]_I + \left\{ \left[\frac{D\mathbf{u}}{Dt} \right]_I - \left[\frac{D}{Dt} (\mathbf{V}_0 + \boldsymbol{\Omega} \times \mathbf{x}) \right]_I \right\} \cdot (\mathbf{V}_0 + \boldsymbol{\Omega} \times \mathbf{x}) \\ &= \mathbf{u}_* \cdot \left[\frac{D}{Dt} (\mathbf{V}_0 + \boldsymbol{\Omega} \times \mathbf{x}) \right]_I + \left\{ \frac{1}{\rho} (-\nabla p + \nabla \cdot \mathbf{T}) - \left[\frac{D}{Dt} (\mathbf{V}_0 + \boldsymbol{\Omega} \times \mathbf{x}) \right]_I \right\} \cdot (\mathbf{V}_0 + \boldsymbol{\Omega} \times \mathbf{x}) \\ &= \mathbf{u}_* \cdot \left[\frac{D}{Dt} (\mathbf{V}_0 + \boldsymbol{\Omega} \times \mathbf{x}) \right]_I + \frac{1}{\rho} (-\nabla p + \nabla \cdot \mathbf{T}) \cdot (\mathbf{V}_0 + \boldsymbol{\Omega} \times \mathbf{x}) - \left[\frac{D}{Dt} (\mathbf{V}_0 + \boldsymbol{\Omega} \times \mathbf{x}) \right]_I \cdot (\mathbf{V}_0 + \boldsymbol{\Omega} \times \mathbf{x}) \\ \text{v.} \quad \frac{1}{2} \left[\frac{D}{Dt} \{ (\mathbf{V}_0 + \boldsymbol{\Omega} \times \mathbf{x}) \cdot (\mathbf{V}_0 + \boldsymbol{\Omega} \times \mathbf{x}) \} \right]_I &= \left[\frac{D}{Dt} (\mathbf{V}_0 + \boldsymbol{\Omega} \times \mathbf{x}) \right]_I \cdot (\mathbf{V}_0 + \boldsymbol{\Omega} \times \mathbf{x}) \end{aligned}$$

Substituting relations ii, iii, iv and v for Eq. (2.9) with rearrangement leads to

$$\rho \frac{D(E^*/\rho)}{Dt} = -\nabla \cdot (p\mathbf{u}_*) + \nabla \cdot (\mathbf{T} \cdot \mathbf{u}_*) - \nabla \cdot \mathbf{q} - \rho \mathbf{u}_* \cdot \left\{ \frac{d\mathbf{V}_0}{dt} + \boldsymbol{\Omega} \times \mathbf{u}_* + \boldsymbol{\Omega} \times (\boldsymbol{\Omega} \times \mathbf{x}) + \frac{d\boldsymbol{\Omega}}{dt} \times \mathbf{x} \right\}$$

Since $\mathbf{u}_* \cdot (\boldsymbol{\Omega} \times \mathbf{u}_*) = 0$, we obtain the energy equation in the moving-coordinate system:

$$\begin{aligned} \rho \frac{D(E^*/\rho)}{Dt} = & -\nabla \cdot (p\mathbf{u}_*) + \nabla \cdot (\mathbf{T} \cdot \mathbf{u}_*) - \nabla \cdot \mathbf{q} \\ & - \rho \mathbf{u}_* \cdot \left\{ \frac{d\mathbf{V}_0}{dt} + \boldsymbol{\Omega} \times (\boldsymbol{\Omega} \times \mathbf{x}) + \frac{d\boldsymbol{\Omega}}{dt} \times \mathbf{x} \right\} \end{aligned} \quad (2.14)$$

In this section, the governing equations of fluid are derived for the general moving-coordinate method: the mass conservation equation, the equation of motion and the energy equation. The latter two equations have the structure where the source terms are added to the ordinary conservation laws.

3 Computational methods

3.1 Computational model

In this study, the parachute is modeled by the two-dimensional, rigid and rectangular concave to aim for grasping basic phenomena. Here shown is the moving-coordinate system only rotating, although we derived that with the fully general case translating and rotating.

Figures 3.1 shows the computation model. We observe the flow field from the xy coordinate system (the moving-coordinate system) that is attached to the moving body and has the origin at the center of rotation. When the body rotates as Figure 3.1 (a) in the standard coordinate system, the moving body stands still as Figure 3.1 (b) if we observe the flow field from the moving-coordinate system.

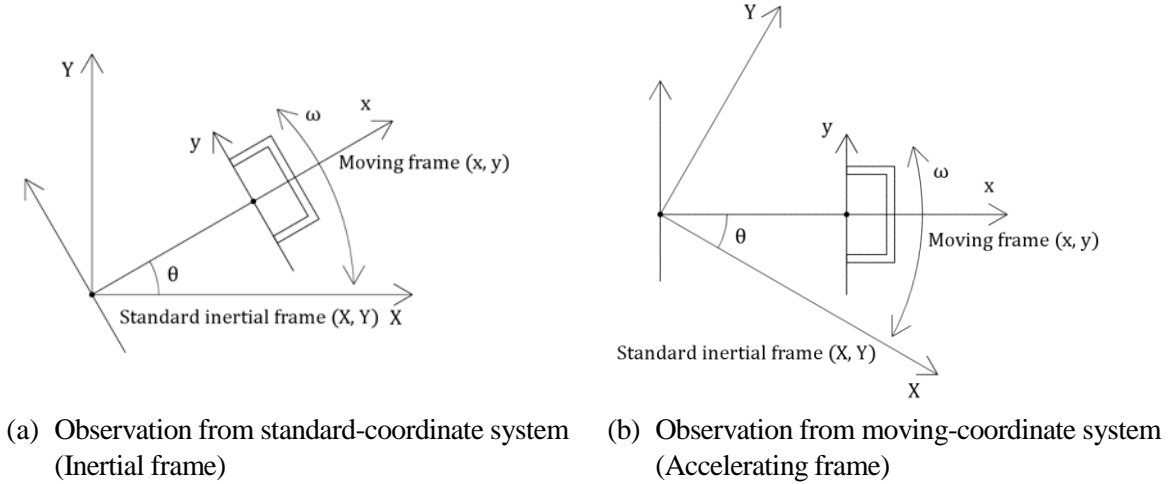


Figure 3.1: Computational models

3.2 Governing equation system and numerical scheme

In the moving-coordinate methods, the two-dimensional, compressible Navier–Stokes equations are expressed in the differential form as follows:

$$\frac{\partial U}{\partial t} + \frac{\partial(F - Re^{-1}F_v)}{\partial x} + \frac{\partial(G - Re^{-1}G_v)}{\partial y} = S \quad (3.1)$$

$$U = \begin{bmatrix} \rho \\ \rho u \\ \rho v \\ E \end{bmatrix}$$

$$F = \begin{bmatrix} \rho u \\ \rho u^2 + p \\ \rho uv \\ (E + p)u \end{bmatrix}, \quad F_v = \begin{bmatrix} 0 \\ \tau_{xx} \\ \tau_{xy} \\ \tau_{xx}u + \tau_{xy}v + \frac{1}{Pr(\gamma - 1)} \left(\kappa \frac{\partial a^2}{\partial x} \right) \end{bmatrix}$$

$$G = \begin{bmatrix} \rho v \\ \rho v^2 + p \\ \rho vu \\ (E + p)v \end{bmatrix}, \quad G_v = \begin{bmatrix} 0 \\ \tau_{yx} \\ \tau_{yy} \\ \tau_{yx}u + \tau_{yy}v + \frac{1}{Pr(\gamma - 1)} \left(\kappa \frac{\partial a^2}{\partial y} \right) \end{bmatrix}$$

$$\tau_{xx} = (\mu + \mu_{sgs}) \left\{ -\frac{2}{3} \left(\frac{\partial u}{\partial x} + \frac{\partial v}{\partial y} \right) + 2 \frac{\partial u}{\partial x} \right\} - \frac{2}{3} \rho k$$

$$\tau_{xy} = \tau_{yx} = (\mu + \mu_{sgs}) \left(\frac{\partial u}{\partial y} + \frac{\partial v}{\partial x} \right)$$

$$\tau_{yy} = (\mu + \mu_{sgs}) \left\{ -\frac{2}{3} \left(\frac{\partial u}{\partial x} + \frac{\partial v}{\partial y} \right) + 2 \frac{\partial v}{\partial y} \right\} - \frac{2}{3} \rho k$$

$$S = \begin{bmatrix} 0 \\ \rho \left(\omega^2 x + 2\omega v + y \frac{d\omega}{dt} \right) \\ \rho \left(\omega^2 y - 2\omega u - x \frac{d\omega}{dt} \right) \\ \rho \left(\omega^2 ux + \omega^2 vy - vx \frac{d\omega}{dt} + uy \frac{d\omega}{dt} \right) \end{bmatrix}, \quad x = x' + l_0$$

$$\text{Equation of state: } p = (\gamma - 1) \left\{ E - \frac{1}{2} \rho (u^2 + v^2) \right\}$$

where $O' - x'y'$ is the coordinate axes on the body with origin O' at the central point of the front end of the body, $O - xy$ is the moving-coordinate system with origin O at the center of rotation that is obtained by translating the origin from O' to O by l_0 in $-x'$ direction (see Figure 3.2). U is the vector of conservative variables, F and G are the inviscid flux vectors in x and y , F_v and G_v are the viscous flux vectors in x and y , and S is the source term vector appearing in the moving frame.

The balance of moment about the center of rotation is written as follows (see Figure 3.2):

$$I \frac{d^2\theta}{dt^2} = l_g F_t \quad (3.2)$$

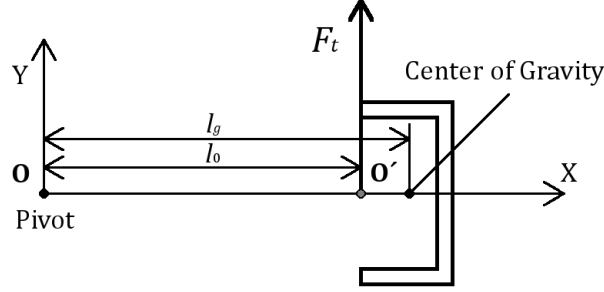


Figure 3.2: Rotating system.

where I is the moment of inertia for the concave body, θ is the rotation angle of the body in standard-coordinate system (See Figure 3.1), l_g is the length between the pivot O and the center of gravity of the body, l_0 is the length between the pivot O and the origin O' of the coordinate axes on the body (the front end of the body), and F_t is the fluid force tangential to the motion of the body.

In general description, momentum $\rho\mathbf{u}$ and total energy E are exchanged from the standard-coordinate system I to the moving-coordinate system A by using Eqs. (2.1) and (2.12):

$$(\rho\mathbf{u})_A = (\rho\mathbf{u})_I - \rho(\mathbf{V}_0 + \boldsymbol{\Omega} \times \mathbf{x}) \quad (3.3)$$

$$E_A = E_I - \rho\mathbf{u}_I \cdot (\mathbf{V}_0 + \boldsymbol{\Omega} \times \mathbf{x}) + \frac{1}{2}\rho(\mathbf{V}_0 + \boldsymbol{\Omega} \times \mathbf{x}) \cdot (\mathbf{V}_0 + \boldsymbol{\Omega} \times \mathbf{x}) \quad (3.4)$$

Similarly, they are exchanged from the moving-coordinate system A to the standard coordinate system I by:

$$(\rho\mathbf{u})_I = (\rho\mathbf{u})_A + \rho(\mathbf{V}_0 + \boldsymbol{\Omega} \times \mathbf{x}) \quad (3.5)$$

$$E_I = E_A + \rho\mathbf{u}_A \cdot (\mathbf{V}_0 + \boldsymbol{\Omega} \times \mathbf{x}) + \frac{1}{2}\rho(\mathbf{V}_0 + \boldsymbol{\Omega} \times \mathbf{x}) \cdot (\mathbf{V}_0 + \boldsymbol{\Omega} \times \mathbf{x}) \quad (3.6)$$

Eq. (3.1) is numerically solved by the finite-volume method, where the third-order TVD Runge-Kutta method is used for the time integration, the inviscid fluxes are evaluated by the seventh-order WENO scheme [12] with the HLLC flux Riemann solver, the viscous fluxes are evaluated by the second-order central difference, and the sub-grid scale Smagorinsky turbulence model are adopted. To obtain θ and $\omega = d\theta/dt$, the time integration is carried out by the Runge-Kutta method.

3.3 Boundary conditions

When the body does not rotate, inlet boundary conditions are set as follows:

$$\rho_{in} = 1.0$$

$$p_{in} = \frac{1.0}{\gamma}$$

$$\begin{pmatrix} u \\ v \end{pmatrix}_{\infty} = \begin{pmatrix} M_{\infty} \\ 0 \end{pmatrix}_{I, \theta=0}$$

Outlet boundary conditions are set as follows: ρ , ρu and ρv are extrapolated with the zeroth-order. If the flow is supersonic ($M \geq 1$), E is extrapolated with the zeroth-order, and if it is subsonic ($M < 1$), E is calculated by using the back pressure value p_{out} given and the extrapolated values of ρ , u , v .

$$E = \frac{p_{out}}{\gamma - 1} + \frac{1}{2}\rho(u^2 + v^2)$$

When the body rotate, inlet boundary conditions are set as follows by using Eqs. (3.3) and (3.4):

$$\rho_{in} = 1.0$$

$$p_{in} = \frac{1.0}{\gamma}$$

$$\begin{pmatrix} u \\ v \end{pmatrix}_{*, \infty} = \begin{pmatrix} M_{\infty} \cos \theta + \omega y \\ -M_{\infty} \sin \theta - \omega x \end{pmatrix}$$

$$E_{*, \infty} = E + \rho\omega\{M_{\infty}(x \sin \theta + y \cos \theta)\} + \frac{1}{2}\rho\omega^2(x^2 + y^2)$$

Outlet boundary conditions are evaluated, according to whether the flow is supersonic or subsonic in the standard-coordinate system: first, physical quantities at the boundary are transformed from the moving-coordinate system to the standard-coordinate system by using Eqs. (3.5) and (3.6); ρ , ρu and ρv are extrapolated with the zeroth-order; if $M \geq 1$, E is extrapolated with the zeroth-order, and if $M < 1$, E is calculated by using the back pressure given and the extrapolated values of ρ , u , v ; after the above settings, the boundary values are transformed back to the moving coordinate system by using Eqs. (3.3) and (3.4).

In the moving-coordinate method, boundary conditions on the wall surface of the body are same as the case of a stationary object with the wall velocity of zero.

4 Computational conditions

Figures 4.1 (a) and (b) show the grid view for the whole computational domain and the enlarged view around the concave body surrounded by the yellow line as a parachute model, respectively. x -directional length inside the body is taken as the characteristic length, so that the length is unity on the grid in Fig. 4.1 (b). The number of grid is 485 in x -direction and 532 in y -direction, so that the detached shock wave should be located within the fine grid region surrounded by the red line in the vicinity of the body in Fig. 4.1 (a).

The left side of the domain is the inlet boundary, and the right, upper and lower sides of the domain are treated as the outlet boundary. The Reynolds number is based on the characteristic length and the speed of sound in the uniform flow, and values of $Re = 1.0 \times 10^5$ and $M_{\infty} = 3.0$ are used in computations. The length between the pivot and the origin of the coordinate axes on the body is set to 15.

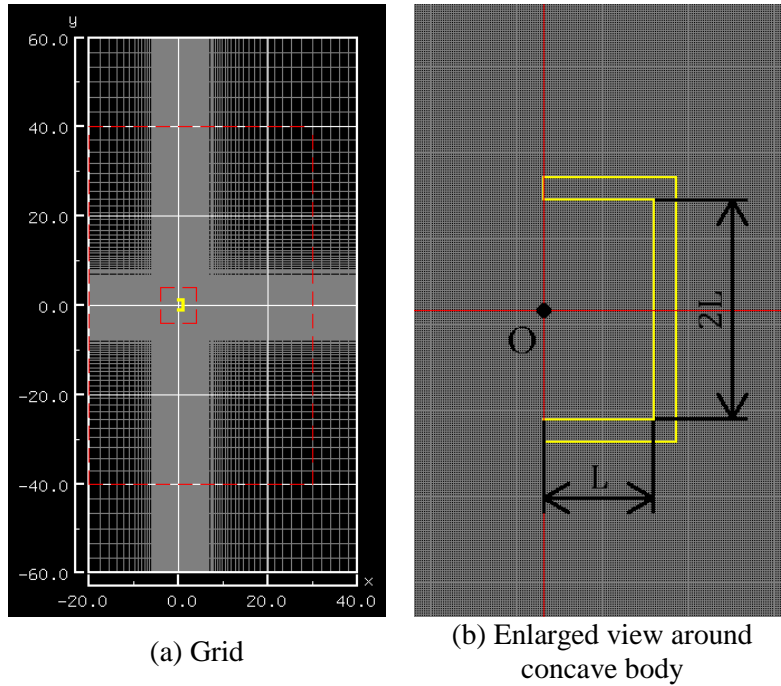
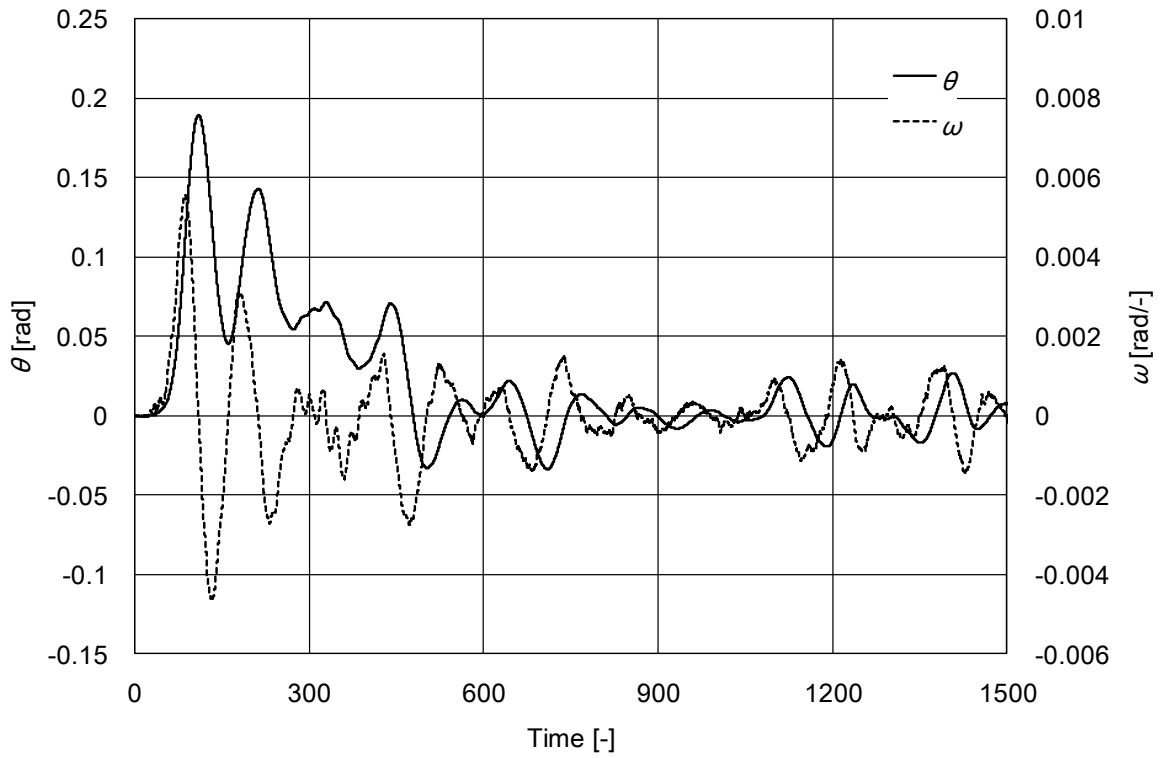


Figure 4.1: Grid and concave body

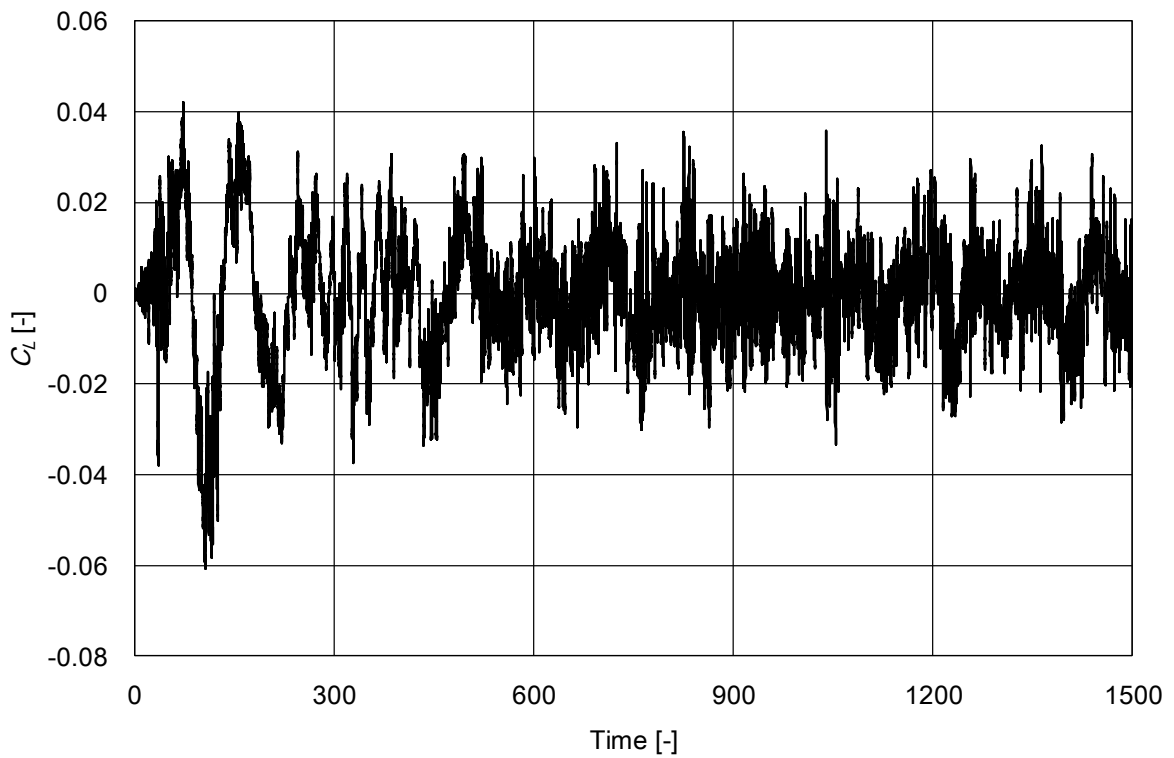
5 Computational Results

Figures 5.1 (a) and (b) show time histories of information about the rotational motion of the body, θ and ω , and the lift coefficient, C_L , respectively. Figure 5.1 (a) shows that it takes about 1100 in non-dimensional time until appropriate flow fields are generated, starting from the initial state including incompatibilities; after about 1100 in time, a self-excited motion is induced physically. In the lift oscillations after about 1100 in time it is observed in Fig. 5.1 (b) that waves with high frequencies may be added to characteristics of the body motion with low frequencies.

Figures 5.2 (a) to (i) show the pressure contours at each time during one period in the self-sustained motion induced in the supersonic flow with $M_\infty = 3.0$. The pressure distributions are those in the standard coordinates transformed from the moving coordinates. Thus moving-coordinate method presented here was applied to the supersonic flow around a parachute-like body, and self-excited motions of the body were captured.



(a) Rotational motion of body: θ and ω .



(b) Lift coefficient: C_L .

Figure 5.1: Time histories for rotational motion of body and coefficient of lift.

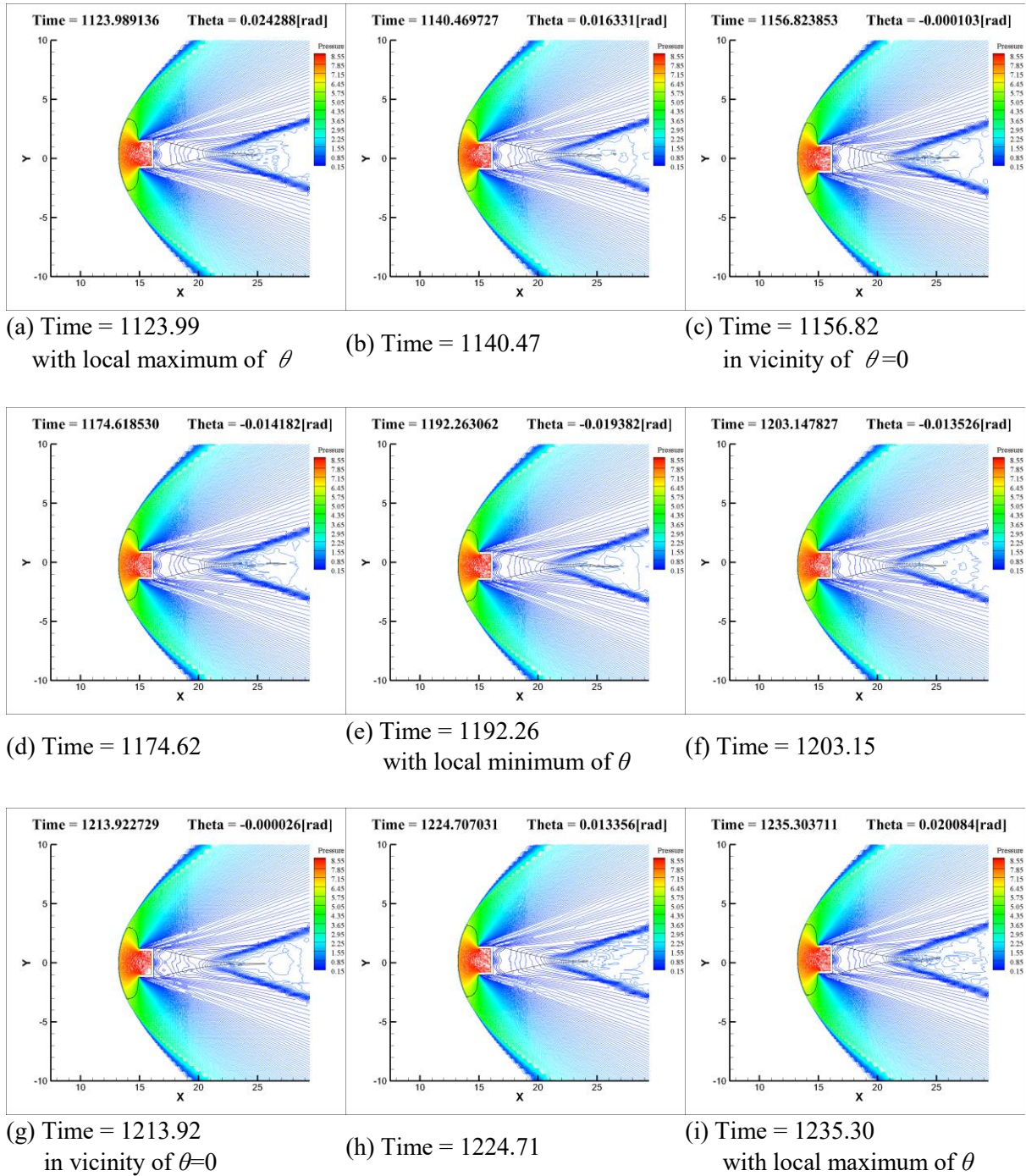


Figure 5.2: Pressure contours around body.

6 Conclusion

The moving-coordinate method presented by the authors is a methodology where physical phenomena are observed from the accelerating frame attached to a moving body. In this study, the moving-coordinate method is generalized by newly including both the translational and rotational motions of the frame. In the moving-coordinate method, as the moving body is observed to be stationary, the present method has advantages that there is no regeneration of the grid around the object

and no calculation error induced by moving grids.

The governing equations of fluid are derived for the generalized moving-coordinate method: the mass conservation equation, the equation of motion and the energy equation. The latter two equations have the structure where the source terms are added to the ordinary conservation laws. Further, the transformations of momentum and total energy between the inertial frame and moving frame are presented. Moreover, the boundary conditions are shown to perform numerical computations on a moving body in supersonic flow fields.

Thus present method was applied to supersonic flows around a parachute-like body, and the self-excited motions of the body were captured.

References

- [1] K. Hiraki. Experimental Study on Aerodynamic Characteristics of Hemisphere Shell in Supersonic Flow Fields. Master's thesis, The University of Tokyo, Japan, 1992.
- [2] T. Kawamura and T. Mizukaki. Aerodynamic Vibrations Caused by a Vortex ahead of Hemisphere in Supersonic Flow. 20th ISSW, 2011.
- [3] Yoko Takakura, Hidetatsu Hiraki, and Norio Arai. On the Flow Fields around a Concave Body in Supersonic Flows. Proceedings of 41st Fluid Dynamics Conference / Aerospace Numerical Simulation Symposium 2009. 2009.
- [4] Akihiko Ozaki, Risa Toyosato and Yoko Takakura. Highly-accurate Computation of Supersonic Flows around a Concave Body. Proceedings of 46th Fluid Dynamics Conference / 32nd Aerospace Numerical Simulation Symposium. JAXA-SP-14-010, 2015.
- [5] R. Toyosato. Vibration Characteristics on Supersonic Flows around a Body. Master's thesis, Tokai University, Japan, 2015.
- [6] K. Hatanaka, S. M. V. Rao, T. Saito, and T. Mizukaki. Numerical investigations on shock oscillations ahead of a hemispherical shell in supersonic flow. Shock Waves, 2016.
- [7] M. Yamakawa and K. Matsuno. An Iterative Finite-Volume Method on an Unstructured Moving Grid (1st Report, The Fundamental Formulation and Validation for Unsteady Compressible Flows). Transactions of the Japan Society of Mechanical Engineers Series B, vol. 69, no. 683, pp. 1577-1582, 2003.
- [8] T. Inomoto, K. Matsuno and M. Yamakawa. Unstructured Moving-Grid Finite-Volume Method for Incompressible Flows and Its Application to a Coupled Problem of Fluid-Dynamics and Body Motion. Transactions of the Japan Society for Computational Engineering and Science, vol. 2015, pp. 20150008, 2015.
- [9] Y. Takakura, F. Higashino, and S. Ogawa. Unsteady flow computations on a flying projectile within a ballistic range. Computers and Fluids, vol. 27, no. 5–6, pp. 645–650, 1998.
- [10] Y. Takakura. Methods for Computing Flows with Moving Boundaries: Governing Equations, Geometric Conservation Laws, and Applications of Moving Coordinate Method. Journal of Japan Society of Computational Fluid Dynamics, vol. 8, no. 3, pp. 117-129, 2000.
- [11] J. H. Spurk. *Fluid Mechanics: Chap.2*, Springer, 1997.
- [12] C.W. SHU. Essentially Non-Oscillatory and Weighted Essentially Non-Oscillatory Schemes for Hyperbolic Conservation Laws. ICASE Report No.97-65, 1997.